一般セッション(口頭講演) | 10 スピントロニクス・マグネティクス：10.1 新物質・新機能創成（作製・評価技術）

2023年9月19日(火) 13:30 ~ 18:00 | C501 (国際交流会館)

[19p-C501-1~16] 10.1 新物質・新機能創成（作製・評価技術）

関 剛斎(東北大)、 安藤 裕一郎(京大)、 磯上 慎二(物材機構)

13:30 ~ 13:45

[19p-C501-1] 組成傾斜磁性ガーネット膜におけるFMR及びMOKE測定

〇大森 康智[1]、染谷 浩子[1]、石田 真彦[1] (1.NEC)

英語発表

13:45 ~ 14:00

[19p-C501-2] High-throughput analysis of compositional dependent magnetoresistance and spin-transfer torque in combinatorially sputtered Co_xFe_{1-x} ($0 \leq x \leq 1$) thin film

〇(PC)Vineet Barwal[1], Hirofumi Suto[1], Tomohiro Taniguchi[2], Yuya Sakuraba[1] (1.NIMS, 2.AIST)

14:00 ~ 14:15

[19p-C501-3] Estimation of a parameter from a metastable magnetic image by machine learning

〇田辺 賢士[1]、久野 栞[1]、出口 慎治[1]、粟野 博之[1] (1.豊田工大)

英語発表

14:15 ~ 14:30

[19p-C501-4] Quantitative measurement of the thermal Hall effect based on magnetic-field-modulated lock-in thermography

〇Takumi Imamura[1,2], Koichi Oyanagi[3,2], Takamasa Hirai[2], Ryo Iguchi[2], Kenta Takamori[3], Satoru Kobayashi[3], Ken-ichi Uchida[1,2] (1.Univ. of Tsukuba, 2.NIMS, 3.Iwate Univ.)

英語発表

14:30 ~ 14:45

[19p-C501-5] High-throughput Calculation of Transverse Transport Properties in Heusler Compounds

〇(P)Guangzong Xing[1], Keisuke Masuda[1], Terumasa Tadano[1], Yoshio Miura[1] (1.NIMS)

奨励賞エントリー 英語発表

15:00 ~ 15:15

[19p-C501-6] Combinatorial optimization for high spin polarization in Heusler alloy composition-spread thin films by anisotropic magnetoresistance effect

〇Ryo Toyama[1], Varun Kumar Kushwaha[1,2], Taisuke Sasaki[1], Yuma Iwasaki[1], Tomoya Nakatani[1], Yuya Sakuraba[1] (1.NIMS, 2.Tohoku Univ.)

奨励賞エントリー 英語発表

15:15 ~ 15:30

[19p-C501-7] Evaluation of spin-mixing conductance in ordered off-stoichiometric $Co_2FeGa_{0.5}Ge_{0.5}$

〇(DC)Madhav Mohan Bhat[1], Hirofumi Suto[2], Yoshio Miura[2], Taisuke Sasaki[2], Alagarsamy Perumal[1], A Srinivasan[1], Yuya Sakuraba[2] (1.IITG, 2.NIMS)

奨励賞エントリー 英語発表

15:30 ~ 15:45

[19p-C501-8] Crystalline structure, magnetic and magnetotransport properties of Mn_3Sn thin films with various thicknesses

〇Shun Wakabayashi[1,2], Ju-young Yoon[1,2], Katarzyna Gas[3,4], Yutaro Takeuchi[5], Yuta Yamane[1,6], Tomohiro Uchimura[1,2], Yuma Sato[1,2], Keisuke Kishi[1,2], Shun Kanai[1,2,3,5,7,8,9], Maciek Sawicki[4], Hideo Ohno[1,3,5,10], Shunsuke Fukami[1,2,3,5,10,11] (1.RIEC, Tohoku Univ., 2.Grad. School of Eng., Tohoku Univ., 3.CSIS, Tohoku Univ., 4.Inst. of Physics, PAS, 5.WPI-AIMR, Tohoku Univ., 6.FRIS, Tohoku Univ., 7.PRESTO, JST, 8.DEFS, Tohoku Univ., 9.QST, 10.CIES, Tohoku Univ., 11.InaRIS)

英語発表
15:45 ~ 16:00

[19p-C501-9] Topological aspects of the anomalous transport phenomena in amorphous Fe–Sn thin films

〇Kohei Fujiwara[1], Yasuyuki Kato[2], Hitoshi Abe[3,4,5], Shun Noguchi[1], Junichi Shiogai[1], Yasuhiro Niwa[3,4], Hiroshi Kumigashira[3,6], Yukitoshi Motome[2], Atsushi Tsukazaki[1,7] (1.IMR, Tohoku Univ., 2.Univ. Tokyo, 3.IMS, KEK, 4.SOKENDAI, 5.Ibaraki Univ., 6.IMRAM, Tohoku Univ., 7.CSIS, Tohoku Univ.)

16:00 ~ 16:15

[19p-C501-10] 立方晶系Fe_3Sn薄膜の規則度と物性評価

相川 皆子[1]、大石 舜士[1]、島田 敏宏[1]、〇長浜 太郎[2]、増田 啓介[3]、桜庭 裕弥[3] (1.北大総化、2.山口大工、3.NIMS)

英語発表
16:15 ~ 16:30

[19p-C501-11] Scaling of the anomalous Hall effect of MBE-grown Cr_2Te_3 thin films

〇Yujun Wang[1], Kawaguchi Masashi[1], Shunzhen Wang[1], Jun Uzuhashi[2], Tadakatsu Ohkubo[2], Masamitsu Hayashi[1] (1.The Univ. of Tokyo, 2.NIMS)

英語発表
16:45 ~ 17:00

[19p-C501-12] Correlation between magnetostriction and magnetic damping in nitride films

〇Keita Ito[1], Ivan Kurniawan[2], Yoshio Miura[2], Yasushi Endo[3], Takeshi Seki[1] (1.IMR, Tohoku Univ., 2.NIMS, 3.Grad. Sch. Eng., Tohoku Univ.)

英語発表
17:00 ~ 17:15

[19p-C501-13] Analyzing magnetic structures of $Mn_{4-x}Ge_xN$ films using x-ray magnetic dichroism measurement

〇Tomohiro Yasuda[1], Kenta Amemiya[2], Kaoru Toko[1], Takashi Suemasu[1] (1.Univ. of Tsukuba, 2.KEK IMSS)

英語発表
17:15 ~ 17:30

[19p-C501-14] Epitaxial growth of several nm-thick Mn_4N film on MgO(001) with Pt buffer layer

〇Takumi Horiuchi[1], Tomohiro Yasuda[1], Aoi Hatate[1], Kaoru Toko[1], Takashi Suemasu[1] (1.Univ. of Tsukubad)

英語発表
17:30 ~ 17:45
[19p-C501-15] Demonstration of magnetic compensation at room temperature in $Mn_{4-x}Cu_xN$ epitaxial films
〇(M1)Aoi Hatate[1], Kenta Amemiya[2], Kaoru Toko[1], Takashi Suemasu[1] (1.Univ. of Tsukuba, 2.KEK)

17:45 ~ 18:00
[19p-C501-16] PLD法による(100)MgO上の磁性GdN薄膜の結晶方位制御
〇田中 祐輔[1]、Yoshiharu Krockenberger[1]、国橋 要司[1]、新田 淳作[1,2]、後藤 秀樹[1,3]、眞田 治樹[1] (1.NTT物性研、2.東北大学、3.広島大学)

組成傾斜磁性ガーネット膜における FMR 及び MOKE 測定

FMR and MOKE measurement for composition spread magnetic garnet films

NEC ○大森 康智，染谷 浩子，石田 真彦

NEC Corp. ○Yasutomo Omori, Hiroko Someya Masahiko Ishida,

E-mail: omori_yasu@nec.com

Magnetic garnets (MG) such as Yttrium Iron Garnet (YIG: $Y_3Fe_5O_{12}$) are recently attractive type of magnets for the use of application and also for the stage of research of physical phenomena. Especially the low gilbert damping and strong magneto-optic effects are the important features for the magnetic devices [1]. For instance, it is pointed that YIG dots have potential to be used for probabilistic bit operation [2]. It is essential to find new materials with better properties. However, as there are many candidate of elements and possible processes, it is still challenging to optimize the condition such as the elements, composition ratio, and the shape in the many possible candidates.

In this study, to accelerate the optimization of these conditions, we performed combinatorial experiments for the magnetic garnets. First, we performed combinatorial magnetron sputtering to obtain widely different composition ratio in a single substrate. By using Vector Network Analyzer and semi-auto prober system, we measured the FMR properties of the hundreds samples of different conditions. In the same time the magneto-optic effects were measured for these films. The effect of the composition ratio, doped elements and processes will be discussed at the presentation.

This work was supported by JST-CREST (JPMJCR20C1).

[1] Y Yang, et al., “Recent advances in development of magnetic garnet thin films for application in spintronics and photonics”, Journal of alloys and Compounds 860 158235 (2021).

[2] T. Makiuchi, et al., “Parametron on magnetic dot: Stable and stochastic operation”, Appl. Phys. Lett. 118, 022402 (2021).

High-throughput analysis of compositional dependent magnetoresistance and spin-transfer torque in combinatorially sputtered Co_xFe_{1-x} ($0 \leq x \leq 1$) thin film

Vineet Barwal[1], Hirofumi Suto[1], Tomohiro Taniguchi[2], and Yuya Sakuraba[1]

[1]Research Center for Magnetic and Spintronic Materials, National Institute for Materials Science (NIMS), Tsukuba, 305-0047, Japan

[2]National Institute of Advanced Industrial Science and Technology (AIST), Research Center for Emerging Computing Technologies, Tsukuba, 305-8568, Japan

E-mail: BARWAL.Vineet@nims.go.jp

We develop high-throughput method for measuring the compositional dependence of magnetoresistance (MR) and spin transfer torque (STT) effects in current-perpendicular-to-plane giant magnetoresistance (CPP-GMR) devices using combinatorially sputtered Co_xFe_{1-x} ($0 \leq x \leq 1$) thin films. Combinatorial sputtering is an experimental tool that increases the throughput of material synthesis and characterization by efficient and systematic exploration of a wide range of compositions [1]. Compared to traditional methods that require the fabrication of individual samples for each composition, combinatorial sputtering facilitates composition dependence study at fine intervals from the devices fabricated on a single substrate.

The CPP GMR devices containing combinatorially sputtered Co_xFe_{1-x} ($0 \leq x \leq 1$) composition-gradient layer as ferromagnetic electrode along with a Cu spacer layer, and a NiFe layer were fabricated. The sample configuration along with combinatorial sputtering process is shown in the figure below. The MR ratio was obtained from resistance versus field measurements in an auto-prober system. The STT efficiency was measured by inducing magnetization reversal of the NiFe layer by spin injection from the Co_xFe_{1-x} layer [2]. The MR ratio and the STT efficiency exhibited a similar trend with respect to the change in composition, having the maximum in the Co concentration range of $0.3 \leq x \leq 0.65$, as shown in the figure. The correlation in the compositional dependence of the MR effect and STT efficiency was theoretically explained by the change in the spin polarization of Co_xFe_{1-x} layer. The large sample size obtained through combinatorial sputtering facilitated comprehensive and efficient analysis, enabling mapping of the composition-property relationship and identify optimal composition of CoFe for spintronic applications.

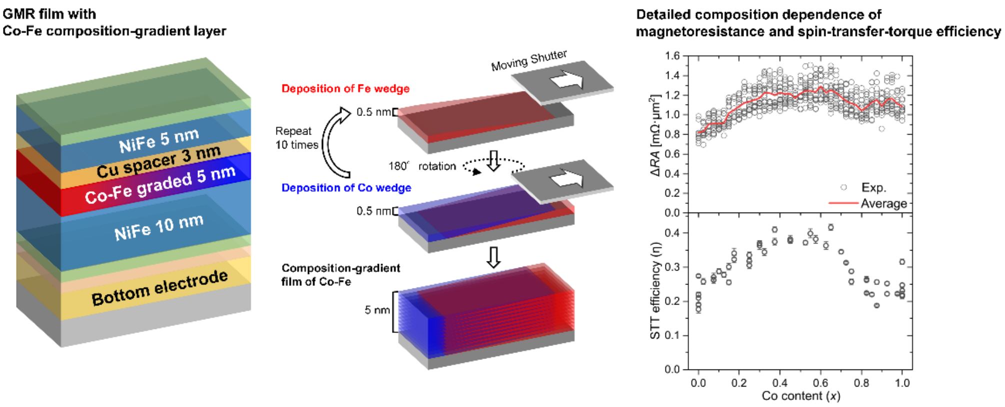

Figure: Sample configuration along with the schematic showing the deposition procedure for the composition gradient layer and compositional dependence of MR and STT

References

[1] R. Modak, K. Goto, S. Ueda, Y. Miura, K. I. Uchida, and Y. Sakuraba, *Combinatorial Tuning of Electronic Structure and Thermoelectric Properties in Co2MnAl1- XSixWeyl Semimetals*, APL Mater. **9**, (2021).

[2] H. Suto, T. Nakatani, N. Asam, H. Iwasaki, and Y. Sakuraba, *Evaluation of Spin-Transfer-Torque Efficiency Using Magnetization Reversal against a Magnetic Field: Comparison of FeCr with Negative Spin Polarization and NiFe*, Appl. Phys. Express **16**, (2023).

Estimation of a parameter from a metastable magnetic image by machine learning

Toyota Technological Institute,
Kenji Tanabe, Shiori Kuno, Shinji Deguchi, and Hiroyuki Awano
E-mail: tanabe@toyota-ti.sc.jp

In the field of magnetism and spintronics, determining material parameters of deposited magnetic films is the most important experiment to evaluate them. Some parameters such as the Dzyaloshinskii–Moriya interaction (DMI) constant, however, are difficult or time-consuming to measure. Therefore, in order to establish a simpler method for estimating parameters, research is being conducted to estimate parameters from magnetic domain images by machine learning[1-3]. In general, ferromagnetic materials have hysteresis in the M-H curve, indicating that the magnetic domain state is not necessarily in the most stable state, but often in a metastable state. In previous studies[1-3], experiments have been conducted with the most stable magnetic state, or without any particular control on whether it is the most stable or metastable state. In this study, we artificially created several metastable states, and conducted to estimate the Tb concentration in TbCo alloy films from the images[4].

Multilayers of Si_3N_4 (10 nm)/$Tb_xCo_{1-x}(t)$/Si_3N_4 (10 nm) were fabricated on Si substrate by sputtering method. Compositions were selected under conditions that resulted in perpendicularly magnetized films, and nine different composition films were fabricated. The AC demagnetization method was used to fabricate the magnetic domain structures. By modulating the rate of decay of the amplitude of the AC magnetic field, multiple metastable states of magnetic domain structures were fabricated (Figure (a)). Figure (b) shows the relationship between the experimentally measured Tb concentration and the value estimated by machine learning. The estimated values are almost proportional to the measured values, suggesting that the Tb concentration can be estimated from the metastable state images.

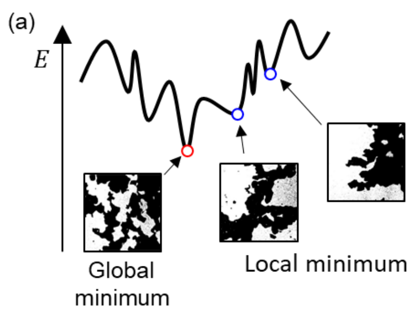

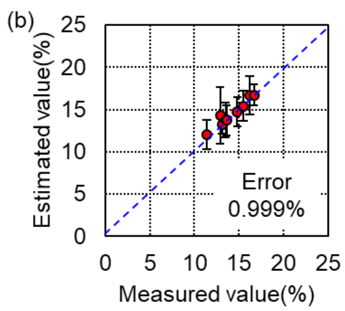

Fig. (a) Images of the most stable and metastable states. In a magnet with hysteresis, the shape of the potential has a multi-valley structure. (b) Relationship between experimentally measured values and values estimated by machine learning. The dotted line is the straight line with slope 1.

[1] D. Wang et al., Advanced Science **7**, 2000566 (2020).
[2] H. Y. Kwon et al., Science Advances **6**, eabb0872 (2020).
[3] M. Kawaguchi, K. Tanabe et al., npj Compu. Mater. **7**, 20 (2021).
[4] S. Kuno, K. Tanabe et al., submitted.

磁場変調型ロックインサーモグラフィに基づく熱ホール効果の定量測定

Quantitative measurement of the thermal Hall effect based on magnetic-field-modulated lock-in thermography

筑波大 [1], NIMS [2], 岩手大 [3]

○今村拓未 [1,2], 大柳洸一 [2,3], 平井孝昌 [2], 井口亮 [2], 髙森健太 [3], 小林悟 [3], 内田健一 [1,2]

Univ. of Tsukuba [1], NIMS [2], Iwate Univ. [3]

°Takumi Imamura [1,2], Koichi Oyanagi [2,3], Takamasa Hirai [2], Ryo Iguchi [2], Kenta Takamori [3], Satoru Kobayashi [3], and Ken-ichi Uchida [1,2]

E-mail: IMAMURA.Takumi@nims.go.jp

The thermal Hall effect (THE) is the thermal analogue of the Hall effect. The measurements of THE are versatile tools for investigating physics of transport properties in a solid since THE is caused not only by electrons but also by phonons and magnons[1]-[5]. THE also has a potential for thermal management technologies because it controls the direction of a heat flow using magnetic fields and/or magnetism. Despite its scientific interest and technological importance, a few experimental studies on THE have been reported so far due to measurement difficulties. The conventional measurements of THE are based on a contact method using temperature sensors, such as thermocouples, attached to a sample, which could reduce the experimental reproducibility and accuracy due to the unavoidable heat leakage from the sample to the sensors. Therefore, the development of simple and quantitative THE measurement methods based on non-contact temperature detection is necessary for further advances in physics investigation and material searching for THE.

Here, we propose and demonstrate a non-contact thermal imaging method for THE based on the magnetic-field-modulated lock-in thermography technique[6]. We visualized the spatial distribution of the temperature change induced by THE in four ferromagnetic conductors, i.e., Ni, $Ni_{70}Pd_{30}$, $Ni_{25}Fe_{75}$, and Co_2MnGa, and quantified their thermal Hall angle. Because the technique established here is applicable to a variety of materials including conductors and insulators, our study will stimulate fundamental physics and materials science studies on THE.

References:

[1] A. W. Smith and A. W. Smith, Phys. Rev. **5**, 35 (1915).

[2] C. Strohm, G. L. J. A. Rikken, and P. Wyder, Phys. Rev. Lett. **95**, 155901 (2005).

[3] Y. Onose, Y. Shiomi, and Y. Tokura, Phys. Rev. Lett. **100**, 016601 (2008).

[4] Y. Onose, T. Ideue, H. Katsura, Y. Shiomi, N. Nagaosa, and Y. Tokura, Science **329**, 297 (2010).

[5] K. Tomioka, K. Uchida, R. Iguchi, and H. Nagano, J. Appl. Phys. **128**, 215103 (2020).

[6] Y. Hirayama, R. Iguchi, X. Miao, K. Hono, and K. Uchida, Appl. Phys. Lett. **111**, 163901 (2017).

High-throughput Calculation of Transverse Transport Properties in Heusler Compounds

NIMS [1], °Guangzong Xing[1], Keisuke Masuda[1], Terumasa Tadano[1], Yoshio Miura[1]

E-mail: Xing.guangzong@nims.go.jp

Improving the performance of transverse thermoelectric devices has attracted significant attention in recent years due to their inherent simplicity compared to conventional longitudinal thermoelectric devices. The transverse electronic and thermal transport properties of a device are evaluated based on the anomalous Hall conductivity σ_{xy} and anomalous Nernst conductivity α_{xy}, respectively. Previous studies [1] have demonstrated that the intrinsic contribution to σ_{xy} is closely linked to the topological properties of the electronic structure, specifically the Berry curvature (BC) characterized by the existence of Weyl nodes or nodal lines in topologically non-trivial Weyl semimetals.

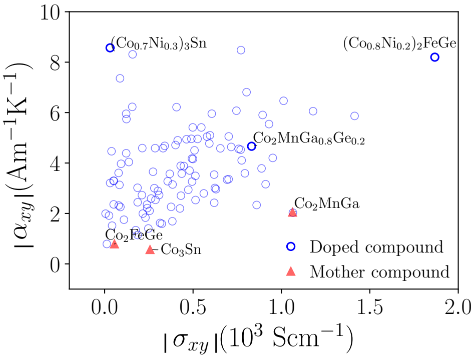

Figure 1. Absolute value of σ_{xy} ($T = 0$ K) and α_{xy} ($T = 300$ K) for magnetic Heusler compounds. Note that the promising doped candidates and mother compounds with large α_{xy} are indicated by empty circles and filled triangles, respectively.

More recently, the $L2_1$-type full Heusler compounds (space group: $Fm\bar{3}m$, formula X_2YZ, where X and Y are transition metals and Z is the main ground element) have been identified as one of the most promising candidates for achieving large values of σ_{xy} and α_{xy}. Noky *et al.* [2] performed a comprehensive study on the intrinsic anomalous transport properties of full Heusler compounds, revealing that the vital role of crystal symmetry in generating substantial net BC for giant σ_{xy} and α_{xy}. However, in their study, the effect of chemical doping on σ_{xy} and $\alpha_{xy}$was not considered directly. Additionally, quaternary Heusler alloys have been extensively studied in experiments for various intriguing physical properties, such as high magnetoresistance ratios in magnetic junctions and current-perpendicular-to-plane giant magnetoresistance devices.

Motivated by these findings, we conducted a comprehensive study aimed at directly investigating the effect of chemical doping on the σ_{xy} and α_{xy} in full Heusler compounds. Our approach involved high-throughput calculations based on density functional theory (DFT) and encompassed a large dataset comprising 1500 ternary and quaternary Heusler compounds. Chemical doping was simulated using the virtual crystal approximation (VCA) approach. Figure 1 illustrates the identification of several doped candidates that exhibit superior α_{xy} compared to the corresponding undoped mother compounds. A detailed analysis revealed that, in certain Heusler compounds, chemical doping can significantly alter the band structure near the Fermi energy, resulting in a large BC, consequently, an enhanced σ_{xy} and α_{xy}.

Reference

[1] D. Xiao, J. Shi, and Q. Niu, *Phys. Rev. Lett.* 95, 137204 (2005)
[2] J. Noky, Y. Zhang, J. Gooth, C. Felser, and Y. Sun, *npj Comput. Mater.* 6, 1-8 (2020)

Combinatorial optimization for high spin polarization in Heusler alloy composition-spread thin films by anisotropic magnetoresistance effect

°R. Toyama,[1] V. K. Kushwaha,[1,2] T. T. Sasaki,[1] Y. Iwasaki,[1] T. Nakatani,[1] and Y. Sakuraba[1]

[1] NIMS, [2] Tohoku University

Email: TOYAMA.Ryo@nims.go.jp

Half-metallic Co-based full-Heusler alloys have been promising candidates for spintronic applications such as tunnel magnetoresistance (TMR) and current-perpendicular-to-plane giant magnetoresistance (CPP-GMR) devices due to their high spin polarization and high Curie temperature [1]. It is shown both theoretically and experimentally that the spin polarization of Heusler alloys strongly depends on the alloy composition [2]. Thus, the optimization of atomic composition of Heusler alloys is crucial for obtaining high spin polarization. However, because of many fabrication steps for those devices, compositional optimization using TMR and CPP-GMR devices is a time-consuming process.

Recently, the measurement of anisotropic magnetoresistance (AMR) effect has been proposed as a facile way to evaluate the spin polarization of Heusler alloys [3]. The magnitude of negative AMR ratio showed a qualitative correlation with the magnitude of GMR for various Heusler alloys, which indicates that a large negative AMR ratio corresponds to a high spin polarization [3].

Combinatorial technique such as using composition-spread films has been widely used for high-throughput material screening. The composition-spread film is the film whose composition changes continuously within a single piece of substrate. By employing the AMR measurement on Heusler alloy composition-spread films, a high-throughput optimization for high spin polarization would be possible.

In this study, we performed a high-throughput compositional optimization method for high spin polarization in Co_2(Mn, Fe)Ge (CMFG) Heusler alloy by a combination of composition-spread films and AMR measurement [4]. From this method, we observed high spin polarization of over 80% at room temperature in polycrystalline $L2_1$-ordered CMFG Heusler alloy thin films on SiO_2/Si substrates. Two types of composition-spread films of $Co_2(Mn_{1-x}Fe_x)Ge$ and $(Co_2Mn_{0.5}Fe_{0.5})_{1-y}Ge_y$ were fabricated by combinatorial sputtering deposition, followed by post-annealing. The compositional dependence of AMR showed the largest negative AMR ratio of –0.13% for y = 0.25 in the $(Co_2Mn_{0.5}Fe_{0.5})_{1-y}Ge_y$ composition-spread film. By measuring spin accumulation signals of nonlocal spin-valve devices, the highest spin polarization of 82% was obtained in the region for y = 0.24. Thus, a clear qualitative correlation between the large negative AMR ratio and high spin polarization was confirmed. The combinatorial optimization method combining composition-spread films and AMR measurement proposed in this study was proved to be an efficient high-throughput strategy for the development of half-metallic Heusler alloys with high spin polarization.

This work was supported by JST CREST (Grant No. JPMJCR21O1) and MEXT Program: Data Creation and Utilization-Type Material Research and Development Project (Digital Transformation Initiative Center for Magnetic Materials; Grant No. JPMXP112271), Japan.

[1] Y. Sakuraba, M. Ueda, S. Bosu, K. Saito, and K. Takanashi, *J. Magn. Soc. Jpn.* **38**, 45 (2014).
[2] K. Moges, Y. Honda, H.-X. Liu, T. Uemura, and M. Yamamoto, *Phys. Rev. B* **93**, 134403 (2016).
[3] Y. Sakuraba, S. Kokado, Y. Hirayama, T. Furubayashi, H. Sukegawa, S. Li, Y. K. Takahashi, and K. Hono, *Appl. Phys. Lett.* **104**, 172407 (2014).
[4] R. Toyama, V. K. Kushwaha, T. T. Sasaki, Y. Iwasaki, T. Nakatani, and Y. Sakuraba, *to be submitted*.

Evaluation of spin-mixing conductance in ordered off-stoichiometric $Co_2FeGa_{0.5}Ge_{0.5}$

Madhav. M. Bhat[1,2], H. Suto[2], Y. Miura[2], T. Sasaki[2], A. Perumal[1], A. Srinivasan[1], Y. Sakuraba[1,2]
[1]Department of Physics, Indian Institute of Technology, Guwahati, 781-039, India.
[2]Research Center for Magnetic and Spintronic Materials, National Institute for Materials Science, Tsukuba, 305-0047, Japan.
E-mail: m.madhav@iitg.ac.in

Introduction:

In spintronics, generating and injecting spin currents is of growing significance[1]. Bilayers containing a ferromagnetic (FM) and nonmagnetic (NM) layers with strong spin-orbit interaction can be suitable way to study the spin pumping through ferromagnetic resonance (FMR) measurement. In spin-pumping, spin current is injected from FM to NM layer, and is quantified by spin mixing conductance ($g^{\uparrow\downarrow}$) [2]. Recent research has focused on studying spin pumping in FM/NM bilayers using high spin polarized Heusler materials due to their low Gilbert damping (α)[3]. We assessed the $g^{\uparrow\downarrow}$ value of off-stoichiometric $Co_2FeGa_{0.5}Ge_{0.5}$ (CFGG) due to the observed low reported α [4].

Experimental Details:

We prepared three kind of structures: CFGG (8-20 nm) single layer, CFGG (8-20 nm)/Pt (10 nm) bilayer, and CFGG (8 nm)/X (0.2nm)/Pt (10 nm) with insertion of X = Cr, Ru, Ta, Cu, and Ni, on the MgO (001) substrate as shown in Fig. 1.

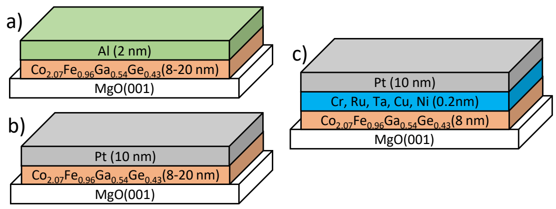

Fig. 1 Schematic representation of sample stack for a) single layer, b) Bilayer, and c) Bilayer with insertion layer.

The samples were in-situ annealed at 600°C for 30 minutes after the deposition of the CFGG layer. The Al passivation layer for the single-layer samples and Pt and X/Pt layers for the bilayer samples were deposited at RT. The CFGG composition was found to be $Co_{51.75}Fe_{25}Ga_{13.5}Ge_{10.75}$ using X-ray fluorescence spectroscopy, and formation of $L2_1$ structure was confirmed using X-ray diffractometer. The α was measured using FMR measurements.

Result and Discussion:

The α values evaluated for the single and bilayer samples revealed a significant increase in α due to spin pumping. The enhancement in α ($\Delta\alpha$) is more pronounced in films with lower ferromagnetic thickness (t_{CFGG}), as shown in Fig. 2.a. The t_{CFGG} dependence of $\Delta\alpha$ was fitted by the following equation to evaluate $g^{\uparrow\downarrow}$.

$$\Delta\alpha = \frac{g\mu_B g^{\uparrow\downarrow}}{4\pi M_s}\frac{1}{t_{CFGG}}$$

Here, $\Delta\alpha$ corresponds to change in damping and $4\pi M_s$ represents the saturation magnetization obtained from VSM measurements.

The evaluated $g^{\uparrow\downarrow}$ for the off-stoichiometric CFGG is (2.85 ± 0.09) x10^{19} m^{-2}. This large value of $g^{\uparrow\downarrow}$ is crucial for applications such as spin transfer torque magnetization switching and spin logic devices.

In Fig. 2.b, the impact of a 0.2 nm insertion layer of Cr, Ru, Ta, Cu, and Ni on the α value is illustrated. As the $\Delta\alpha$ are influenced by interface modifications, we can tune the $g^{\uparrow\downarrow}$.

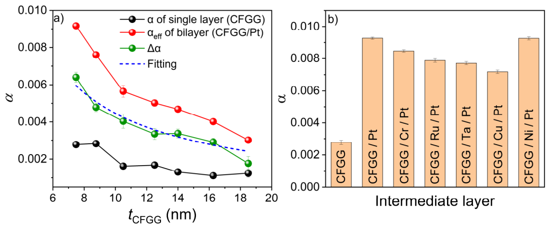

Fig. 2 a) t_{CFGG} dependence α for single-layer and bilayer samples. $\Delta\alpha$ is also shown. b) change in α for different insertion layer.

References

[1] Wolf *et al.*, *Science (80-.).*, vol. 294, no. 5546, pp. 1488–1495, (2001).
[2] Tserkovnyak *et al.*, *Rev. Mod. Phys.*, vol. 77, no. 4, pp. 1375–1421, (2005)
[3] Mizukami *et al.*, *Phys. Rev. B - Condens. Matter Mater. Phys.*, vol. 66, no. 10, pp. 1044131–1044139, (2002)
[4] M.M. Bhat, *et al.*, Manuscript in preparation.

Crystalline structure, magnetic and magnetotransport properties of Mn_3Sn thin films with various thicknesses

°S. Wakabayashi[1,2], J.-Y. Yoon[1,2], K. Gas[3,4], Y. Takeuchi[5], Y. Yamane[1,6], T. Uchimura[1,2], Y. Sato[1,2], K. Kishi[1,2], S. Kanai[1,2,3,5,7,8,9] M. Sawicki,[4] H. Ohno[1,3,5,10] and S. Fukami[1,2,3,5, 10,11]

[1]Laboratory for Nanoelectronics and Spintronics, RIEC, Tohoku Univ., [2]Graduate School of Engineering, Tohoku Univ., [3]CSIS, Tohoku Univ., [4]Institute of Physics, Polish Academy of Sciences, [5]WPI-AIMR, Tohoku Univ., [6]FRIS, Tohoku Univ., [7]PRESTO, JST, [8]DEFS, Tohoku Univ., [9]QST, [10]CIES, Tohoku Univ., [11]InaRIS

E-mail: wakabayashi.shun.s7@dc.tohoku.ac.jp

Non-collinear antiferromagnet $D0_{19}$-Mn_3Sn has attracted much attention owing to its unique physical properties [1,2] and functionalities [3,4]. For further exploration, comprehensive characterization of crystalline structure and magnetic/magnetotransport properties is of great importance. Here, we systematically investigate these fundamental properties of Mn_3Sn thin film as a function of thickness and discuss the correlation between each parameter.

For the sample preparation, we deposit stacks consisting of W (2 nm)/Ta (3 nm)/Mn_3Sn (t_{Mn_3Sn})/MgO (1.3 nm)/Ru (1 nm) on MgO (110) substrate by DC/RF magnetron sputtering with various Mn_3Sn thicknesses t_{Mn_3Sn} ranging in 10-100 nm, followed by annealing at 500 ºC for an hour.

X-ray diffraction reveals that the $(1\bar{1}00)$ oriented epitaxial structure is formed in 20-40 nm, where the lattice parameter a approaches the bulk value as t_{Mn_3Sn} increases; polycrystalline structure is formed above 50 nm; and the order parameter S for $D0_{19}$ structure, rapidly increases from 15 to 20 nm and keeps a constant value of ~0.6 as reported in [5] above 20 nm. Magnetization measurement reveals that the Mn_3Sn layer has a spontaneous magnetization of 4.5±1.0 mT with a magnetically inactive thickness of about 7 nm. Magnetic anisotropy evaluated from a transport measurement shows a dominant contribution of two-fold anisotropy λ_2 that decreases with t_{Mn_3Sn} in the range 20-40nm. The saturated Hall conductivity $\sigma_{\mathrm{H}}^{\mathrm{sat}}$ rapidly increases from 15 to 20 nm and, above 20 nm, it saturates at ~20 Scm^{-1}, which is close to the one reported for a bulk sample [1]. From the obtained results, we infer that λ_2 is correlated with a through the strain as pointed out in a previous report [6] and $\sigma_{\mathrm{H}}^{\mathrm{sat}}$ is affected by a formation of $D0_{19}$ structure. This work is an important step towards developing functional devices based on non-collinear antiferromagnetic thin films.

This work was partly supported by JSPS Kakenhi (Nos. 19H05622, 21J23061, and 22K14558), Casio foundation (No. 40-4), and RIEC Cooperative Research Projects.

[1] S. Nakatsuji et al., Nature **527**, 212 (2015). [2] T. Higo *et al.*, Nat. Photon. **12**, 73 (2018). [3] H. Tsai *et al.*, Nature **580**, 608 (2020). [4] Y. Takeuchi *et al*., Nat. Mater. **20**, 1364 (2021). [5] J.-Y. Yoon *et al*., AIP. Adv., **11**, 065318 (2021). [6] T. Higo, et al., Nature, **607**, 474 (2022).

Topological aspects of the anomalous transport phenomena in amorphous Fe–Sn thin films

IMR, Tohoku Univ. [1], Univ. Tokyo[2], IMS, KEK[3], SOKENDAI[4], Ibaraki Univ.[5],

IMRAM, Tohoku Univ.[6], CSIS, Tohoku Univ.[7]

°K. Fujiwara[1], Y. Kato[2], H. Abe[3,4,5], S. Noguchi[1], J. Shiogai[1], Y. Niwa[3,4], H. Kumigashira[3,6],

Y. Motome[2], and A. Tsukazaki[1,7]

E-mail: kohei.fujiwara@tohoku.ac.jp

The intermetallic ferromagnetic compounds Fe_3Sn_2 and Fe_3Sn, which are characterized by Fe kagome lattices, exhibit large anomalous Hall effect (AHE) and anomalous Nernst effect (ANE) at room temperature, respectively [1,2]. As the origin of these large responses, the contribution of Berry curvature originating from the band singularities, e.g., Dirac/Weyl points and nodal lines, has been discussed. Since the crystal-lattice symmetry as well as spin-orbit coupling is understood to play an essential role in forming such band singularities, amorphous materials lacking long-range crystalline order have thus far been out of the scope of the materials search in this trend. However, we have reported that in amorphous-like $Fe_{0.6}Sn_{0.4}$ thin films sputter-deposited at room temperature, a large AHE comparable to that of Fe_3Sn_2 bulk single crystals occurs, although most of the films lack features of the long-range crystalline order [3]. In this study, using more uniformly amorphous Fe_xSn_{1-x} thin films, we have clarified the topological aspects of short-range kagome-lattice order hidden in the amorphous by experiments and model calculations [4].

Fe_xSn_{1-x} films were deposited on glass substrates by co-sputtering at room temperature. The films were categorized to be amorphous within conventional X-ray diffraction and transmission electron microscopy as shown in Fig. 1(a). Figure 1(b) shows Nernst coefficient S_{xy} versus magnetic field $\mu_0 H$ curves of x = 0.74, where the saturated S_{xy} value exceeding 1.0 μV K^{-1} was observed, comparable to those reported for topological semimetal crystals. Such a large S_{xy} value has been interpreted in the framework of the Berry-curvature-derived intrinsic mechanism. We developed a simulation model based on a short-range kagome-lattice order on the scale of the nearest neighboring atom distances detected by X-ray absorption spectroscopy, revealing that the kagome-lattice fragments contribute to the large AHE and ANE via the intrinsic mechanism.

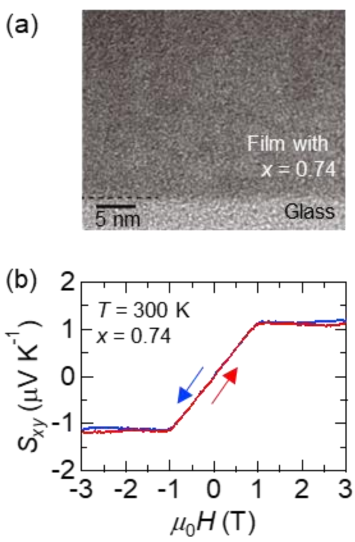

Fig. 1. (a) Transmission electron microscopy image of x = 0.74. (b) S_{xy} vs $\mu_0 H$ curves of x = 0.74 measured by applying an in-plane temperature gradient at T = 300 K.

[1] L. Ye *et al.*, *Nature* **555**, 638 (2018), [2] T. Chen *et al.*, *Sci. Adv.* **8**, eabk1480 (2022), [3] K. Fujiwara *et al.*, *JSAP Rev.* **2023**, 230414 (2023), [4] K. Fujiwara *et al.*, *Nature Commun.* **14**, 3399 (2023).

立方晶系 Fe_3Sn 薄膜の規則度と物性評価

Crystal structure order and physical characteristics of cubic Fe_3Sn thin film

北大総化[1], 山口大工[2] NIMS[3]

相川皆子[1] 大石舜士[1] 島田敏宏[1] ○長浜太郎[2] 増田啓介[3] 桜庭裕弥[3]

Hokkaido Univ.[1], Yamaguchi Univ.[2], NIMS[3]. M. Aikawa[1], S. Ohishi[1],

T. Shimada[1], ○T. Nagahama[2], K. Masuda[3], Y. Sakuraba[3].

E-mail: nagahama@yamaguchi.ac.jp

【背景】近年、熱電発電素子を開発するにあたって、異常ネルンスト効果(ANE)を有する物質が注目されている。とくにトポロジカルな電子状態に起因した巨大な ANE は実用へのブレークスルーになり得ると期待され、Fe_3Al[1], Fe_3Ga[1], Co_2MnAl[2]などの報告がなされた。Fe_3X 系の材料は体心立方構造を基調とした $D0_3$ 構造を有している。我々は MgO 基板上へのエピタキシャル成長によって準安定構造である立方晶 Fe_3Sn 合金薄膜の作成に成功した。この薄膜は強磁性体であり ANE を示すが、その機構・特性など詳細はあきらかでない。本研究では Fe_3Sn の ANE と規則度に着目し、結晶構造と ANE との関連を検討した。

【実験方法】薄膜試料は MBE 法を用いて作製した。基板には MgO(100)を用いて Fe_3Sn 合金薄膜試料の作製を行った。蒸着温度を変えた数種類の試料を作製し、XRD による結晶構造解析、SQUID による磁気特性の測定をおこなった。さらに微細加工によりホールバー形状を作成し、熱電能および磁気抵抗効果・ホール効果などを評価した。

【結果と考察】Fig1 に XRD 測定の結果を示す。200~500 ℃で製膜した試料で 002 ピークが見られ、500 ℃まで蒸着温度の上昇とともに B2 規則度が上昇した。500 ℃で蒸着した薄膜では 111 ピークも観測されたことから部分的に $D0_3$ 構造が形成していると考えられる。また、100 ℃で製膜した試料は多結晶的であった。Fig 2 に異常ネルンスト効果の測定結果を示す。400 ℃製膜の試料に向けて S_{ANE}, α_{xy} といった ANE のパラメータが上昇しており、400 ℃製膜の Fe_3Sn 薄膜試料で SANE =2.3 μ V/K, α_{xy} =1.4 A/mK という最大値を得た。また、500 ℃製膜の Fe_3Sn 薄膜ではどちらの値も下がっていた。これは B2 構造からの結晶構造変化に起因すると考えられる。当日は電子状態計算の結果とあわせて議論する。【参考文献】1. A. Sakai et al. Nature 581, 53–57 (2020). 2. Y. Sakuraba et al., Phys. Rev. B 101, 134407 (2020). 3. Y. Goto et al., Jpn. J. Appl. Phys. 57 120302 (2018).

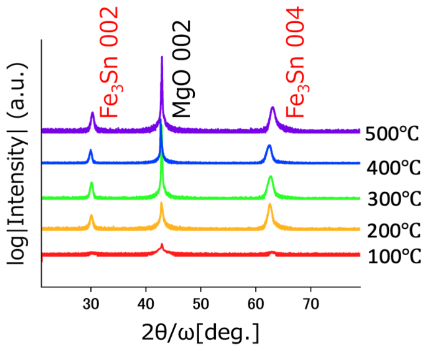

Fig.1. Growth temperature dependence of XRD profiles for Fe_3Sn films.

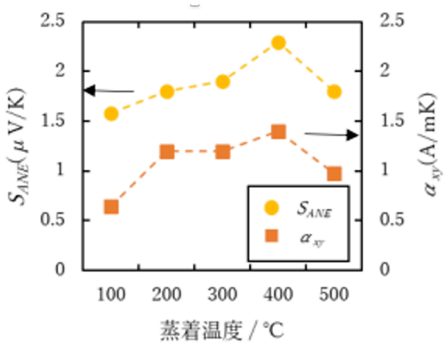

Fig.2. Growth temp. dependence of ANE.

Scaling of the anomalous Hall effect of MBE-grown Cr_2Te_3 thin films

The University of Tokyo [1], National Institute for Materials Science[2],

°Yujun Wang[1], Masashi Kawaguchi[1], Shunzhen Wang[1], Jun Uzuhashi[2], Tadakatsu Ohkubo[2], Masamitsu Hayashi[1]

E-mail: yujun.wang@phys.s.u-tokyo.ac.jp

We performed a systematic study on the magneto-transport properties of Cr_2Te_3 thin films. Cr_2Te_3 is a van der Waals type layered structure with unique ferromagnetic characteristics [1-3]. Studies have shown that the Curie temperature of Cr_2Te_3 can reach room temperature with the increase of film thickness [1]. We have grown Cr_2Te_3 thin films using molecular beam epitaxy (MBE). The film structure is characterized by RHEED, scanning transmission electron microscope (STEM) and X-ray diffraction (XRD). The RHEED patterns show sharp streaks during the growth, indicating the smooth surface of the films. A 2:3 ratio of Cr and Te is confirmed from STEM measurement. Typical Bragg diffraction peaks associated with the hexagonal (0001) planes are observed in XRD spectrum. The position and amplitude of the peaks are in good agreement with tabulated data in the database, suggesting successful preparation of high quality Cr_2Te_3 films.

The magneto-transport properties of the films were studied using micro-fabricated Hall bars. The anomalous Hall resistance R_{AH} is measured against the out of plane magnetic field. A square hysteresis loop is observed at low temperature, indicating the existence of the ferromagnetic phase. The Curie temperature of the films is ~175 K. R_{AH} is found to vary with the measurement temperature. Interestingly, the sign of R_{AH} changes as the temperature is increased. To identify the origin of the sign change, we studied the resistivity ρ_{xx} dependence of R_{AH}. From these results, we discuss possible contributions to the anomalous Hall resistance which causes its sign change. Details of the analysis will be discussed in the presentation.

References: [1] *Li et al.*, ACS Appl. Nano Mater, 2, 6809 (2019). [2] *Lee et al.*, ACS Appl. Nano Mater, 4, 4810 (2021). [3] *Zhong et al.*, Nano Res., 15, 1254 (2022).

Correlation between magnetostriction and magnetic damping in nitride films

IMR, Tohoku Univ.[1], NIMS[2], Grad. Sch. Eng., Tohoku Univ.[3]

°Keita Ito[1], Ivan Kurniawan[2], Yoshio Miura[2], Yasushi Endo[3], Takeshi Seki[1]

E-mail: keita.ito.e3@tohoku.ac.jp

Magnetostrictive materials have been applied to vibration-powered generators and torque sensors, and have attracted attention in recent years for their application to flexible spintronics. A recent paper reported that Fe_4N exhibits a magnetostriction constant of λ_{100} = –75 ppm, which is several times larger than that of typical ferromagnetic metals [1]. Therefore, magnetic nitrides are expected as rare-metal- and rare-earth-free large magnetostrictive materials. However, a material design guideline for further increase of magnetostriction is yet to be clear. In this study, the magnetostriction was investigated for $Fe_{4-x}Mn_xN$ and $Fe_{4-y}Co_yN$ films. The amount of Mn and Co was systematically changed, and we investigated correlation between λ_{100}, saturation magnetization (M_s), magnetic anisotropy constant (K_1), damping constant (α), and density of states at the Fermi level (D). The physical mechanism behind the magnitude of λ_{100} is discussed.

Fe_4N, $Fe_{4-x}Mn_xN$ (x = 0.1, 0.4, 1.0), and $Fe_{4-y}Co_yN$ (y = 0.2, 0.5, 0.8, 1.7, 2.2) films were grown on $SrTiO_3$(001) substrates by molecular beam epitaxy. The structure was characterized by x-ray diffraction and reflection high-energy electron diffraction. λ_{100} was measured by an optical cantilever method. M_s and K_1 were estimated from magnetization curves measured by a vibrating sample magnetometer. α was evaluated by a ferromagnetic resonance method. All the measurements were performed at room temperature.

The epitaxial growth was confirmed for all the Fe_4N, $Fe_{4-x}Mn_xN$, and $Fe_{4-y}Co_yN$ films. The value of λ_{100} showed –110 ppm for the Fe_4N film, exceeding the reported value, and $|\lambda_{100}|$ decreased by adding Mn or Co. Comparing the x and y dependences of $|\lambda_{100}|$, M_s, $|K_1|$, and α, we found a clear positive correlation between $|\lambda_{100}|$ and α. In general, α involves a resistivity-like term and a conductivity-like term [2]. According to the theoretical model [3], the former is expressed as $\alpha \propto \xi^2 D/\tau M_s$ and the latter as $\alpha \propto \xi^2 D\tau/M_s$. ξ is the spin-orbit coupling constant and τ is the relaxation time of electron scattering. If ξ contributes largely as a common term for $|\lambda_{100}|$ and α, a positive correlation should be observed between $|\lambda_{100}|$, α, and $|K_1|$. However, such a correlation is not observed, and only the contribution of ξ cannot explain the positive correlation between $|\lambda_{100}|$ and α. The change of M_s also showed a different trend from that in α. If τ contributes largely as a common term of $|\lambda_{100}|$ and α, and we may assume that the major mechanism of α is based on resistivity-like process, $1/\tau$ dependence of both $|\lambda_{100}|$ and α is expected. This means that τ is short, $|\lambda_{100}|$ is large, and α is large in materials with strong coupling between the lattice system and the spin system. In order to examine the above scenario, we carried out the first-principles calculations to investigate the y dependences of D in $Fe_{4-y}Co_yN$ and the contribution of the conductivity-like term in α, and a guideline for material design to achieve a larger magnetostriction constant will be discussed in the presentation.

[1] Y. Maeda *et al.*, IEICE Technical Report **121**, MRIS2021-7, 6 (2021). [2] S. M. Bhagat and P. Lubitz, Phys. Rev. B **10**, 179 (1974). [3] V. Kamberský, Can. J. Phys. **48**, 2906 (1970).

Analyzing magnetic structures of $Mn_{4-x}Ge_xN$ films using x-ray magnetic dichroism measurement

1. Univ. of Tsukuba, 2. KEK
T. Yasuda[1], K. Amemiya[2], K. Toko[1] and T. Suemasu[1]
E-mail: ytrp108@gmail.com

【Introduction】 Materials based on manganese nitride with antiperovskite crystal structure have been attracted attention thanks to their ferrimagnetic or noncollinear antiferromagnetic structures like, which enable high-speed spin dynamics[1], negative thermal expansion[2], or out-of-plane spin polarization[3]. $Mn_{4-x}Ge_xN$ is also the candidate that show unique magnetic structure with some uncommon physical properties. R. Zhang *et al*. reported MC composition of bulk $Mn_{4-x}Ge_xN$[4]. However, there were no reports on $Mn_{4-x}Ge_xN$ thin films. In this work, we made $Mn_{4-x}Ge_xN$ epitaxial films and performed x-ray absorption spectroscopy (XAS) and x-ray magnetic circular dichroism (XMCD) measurements to investigate the magnetic structures at room temperature.

【Experiment】 We made 20-nm-thick $Mn_{4-x}Ge_xN$ films (x = 0.0, 0.3 and 0.8) on $SrTiO_3$(001) substrates by molecular beam epitaxy. Their epitaxial growths were confirmed by reflection high-energy electron diffraction and x-ray diffraction analysis. XAS and XMCD measurements were conducted by total electron yield method. Both magnetic fields of ±5 T and circularly polarized x-rays were applied perpendicular to sample surface.

【Results】 Figure 1 shows XAS and XMCD spectra on Mn-$L_{2,3}$ absorption edges in $Mn_{4-x}Ge_xN$. XAS spectra did not have composition dependence, indicating that the number of 3d electron in Mn did not change by increasing Ge concentration. In the XMCD spectra of x = 0.0, L_3 edge contains both negative peak α and positive peak β derived from antiparallel magnetic moments in ferrimagnetic Mn_4N structure. Additionally, we find the change in XMCD spectra only between x = 0.0 (Fig. 1(a)) and 0.3 (Fig. 1(b)). From these results, we assume that the magnetic moments of Mn canted each other by doping a small amount of Ge atoms. In my presentation, I will also show the crystallinities and magneto-transport properties of the $Mn_{4-x}Ge_xN$ films.

【Acknowledgement】The XAS and XMCD measurements were performed at BL-16A in KEK-PF (Japan) with the approval of the Photon Factory Program Advisory Committee (Proposal No. 2022G036).

【References】

[1] S. Ghosh *et al*., Nano Lett. 21, 2580 (2021). [2] K. Takenaka *et al*., Sci. Technol. Adv. Mater. 15, 015009 (2014).
[3] Y. You *et al*., Nat. Commun. 12, 6524 (2021). [4] R. Zhang *et al*., Acta Mater. 234, 118021 (2022).

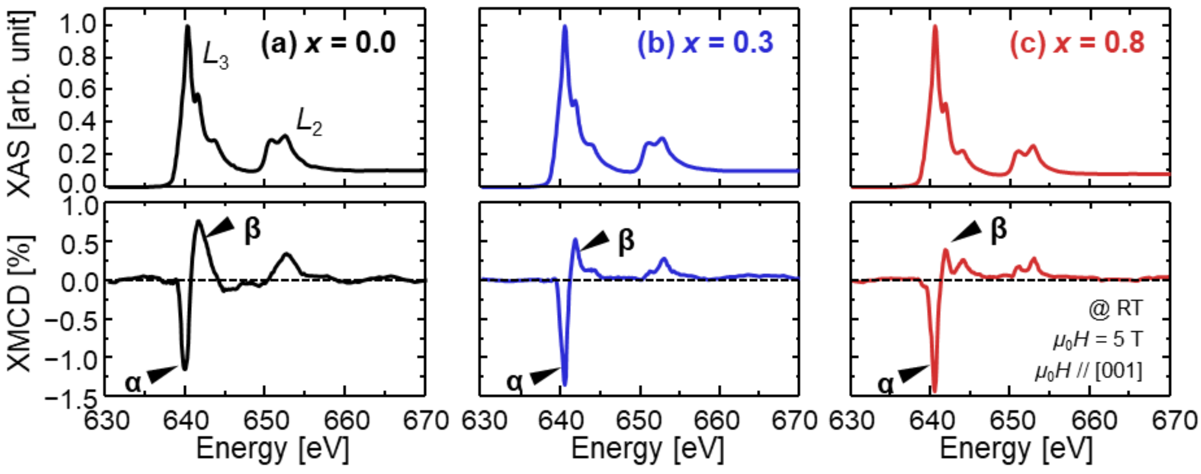

Figure 1. XAS and XMCD spectra of (a) Mn_4N (b) $Mn_{3.7}Ge_{0.3}N$ and (c) $Mn_{3.2}Ge_{0.8}N$ films at Mn-$L_{2,3}$ edges.

Epitaxial growth of several nm-thick Mn_4N film on MgO(001) with Pt buffer layer

1. Univ. of Tsukuba　Takumi Horiuchi[1], T. Yasuda[1], A. Hatate[1], K. Toko[1], and T. Suemasu[1]
E-mail: s2220288@u.tsukuba.ac.jp

[Introduction] Antiperovskite ferrimagnetic Mn_4N film is a candidate for spintronic devices. Its small spontaneous magnetization (M_S ~ 100 kA/m) [1] and perpendicular magnetic anisotropy [2] contributes to rapid and highly efficient domain wall (DW) motion. In our previous research, large DW velocity of 900 m/s (j = 1.3 × 10^{12} A/m^2) was achieved with Mn_4N strips only by spin transfer torque (STT) at room temperature [3]. In addition, Mn_4N film is also expected to be applied to current-induced magnetization switching. There has been previous research which demonstrated spin orbit torque (SOT) switching in the Mn_4N/Pt bilayers through harvesting the spin Hall effect of Pt cap layer [4]. In this work, we attempted to fabricate ultra-thin Mn_4N on Pt/MgO(001) because Dzyaloshinskii-Moriya-interaction at the interface between thin magnetic layer and heavy metal is needed for DW motion by SOT. By using Pt buffer layer, we succeeded the growth of 5-nm-thick Mn_4N films on MgO(001).

[Experiment] We fabricated 8-nm-thick Pt layers onto MgO(001) substrates by sputtering method. Then, we deposited Mn_4N (30nm, 10nm, or 5nm) films on them by molecular beam epitaxy. Their crystalline quality was evaluated by ω–2θ X-ray diffraction (XRD), ω–rocking curve (RC) of XRD, and reflection high-energy electron diffraction (RHEED).

[Result] Figure 1 shows the ω–2θ XRD profiles and RHEED patterns of Mn_4N with and without the Pt buffer layer. We can see only peaks from (001)-oriented planes without ones from (111)-oriented plane. In RHEED patterns, we can see streaks and superlattice diffraction from body-centered nitrogen. In the samples which contain Pt layer, those patterns were sharper.

Figure 2 shows the ω–RC of 30-nm-thick Mn_4N. We confirmed that the FWHM of ω–RC was reduced to less than half by the deposition of Pt buffer layer. It indicates the improvement of the crystallinity by using the Pt buffer layer. From above results, we confirmed the epitaxial growths of Pt and Mn_4N on MgO(001), and improvement of crystalline quality of Mn_4N by the deposition of Pt buffer layer. Magnetic transport properties will be discussed in talk.

[Reference]

[1] T. Gushi *et al.*, Jpn. J. Appl. Phys. **57**, 120310 (2018).
[2] Y. Yasutomi *et al.*, J. Appl. Phys. **115**, 17A935 (2014).
[3] T. Gushi *et al.*, Nano Lett. **19**, 8716 (2019).
[4] H. Bai *et al.*, Adv. Electron. Mater. **8**, 2100772(2022).

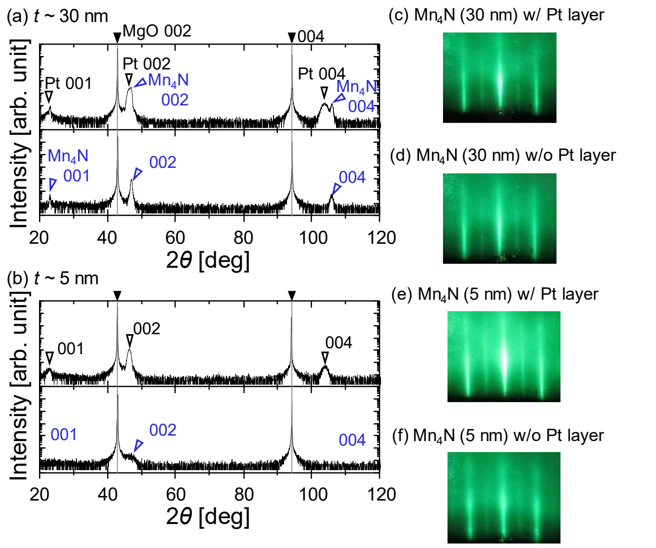

Fig. 1 (a) and (b) ω–2θ XRD profiles of Pt and Mn_4N. (c)–(f) RHEED patterns of Mn_4N with and without Pt layers.

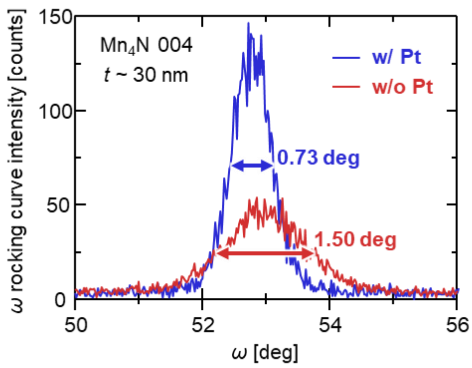

Fig. 2 ω–RC of Mn_4N with and without Pt layers.

Demonstration of magnetic compensation at room temperature in $Mn_{4-x}Cu_xN$ epitaxial films

1. Univ. of Tsukuba, 2. KEK
Aoi Hatate[1], K. Amemiya[2], K. Toko[1], and T. Suemasu[1]
E-mail: blueno.spin@gmail.com

[Introduction] Mn_4N films have a small magnetization and clear perpendicular magnetic anisotropy. Their features are advantageous to new devices using current-induced domain wall (DW) motion. Furthermore, the control of Ni[1] or Co[2] addition into Mn_4N crystals leads to magnetic compensation (MC) at room temperature (RT). At the vicinity of MC composition, an ultrafast DW motion reaching 3,000 m/s (current density 1.2×10^{12} A/m^2) was demonstrated at RT without the help of a magnetic field[3]. This time, we focused on $Mn_{4-x}Cu_xN$ thin films as a new candidate for MC. Although R. Zhang *et al*. reported the possibility of MC in bulk $Mn_{4-x}Cu_xN$ of $x \sim 0.22$ at $T = 4$ K[4], there have been no reports about MC in thin films. We succeeded in the epitaxial growth of high-quality $Mn_{4-x}Cu_xN$ epitaxial films by molecular beam epitaxy (MBE). In addition, we confirmed their MC composition due to the magnetization, X-ray absorption spectra (XAS) and X-ray magnetic circular dichroism (XMCD) measurements. Compensated $Mn_{4-x}Cu_xN$ films are expected to significantly update DW motion efficiency.

[Experiment] 23-nm-thick $Mn_{4-x}Cu_xN$ ($x = 0.0$–0.5) films were epitaxially grown on $SrTiO_3$(001) substrates by MBE. Their saturation magnetizations at RT were measured by a vibrating sample magnetometer. Their magnetic structure was confirmed by XAS and XMCD measurements performed at the twin APPLE-II undulator beamline in KEK-PF (Japan). Both the magnetic field of ± 5 T and circularly polarized X-rays were applied at an incident angle $\theta = 54.7^\circ$ (magic angle). The detection method of Cu is a fluorescence yield method.

[Result] Figure 1 shows the composition dependence of saturation magnetization in $Mn_{4-x}Cu_xN$ thin films. The saturation magnetization at $x = 0.4$ could not be measured because it is too small, having a minimum value between $x = 0.3$ and 0.5. Figure 2 shows XAS and XMCD spectra on Cu-$L_{2,3}$ absorption edges in (a) $Mn_{3.7}Cu_{0.3}N$ and (b) $Mn_{3.6}Cu_{0.4}N$. There was not much difference in the XAS spectra between $x = 0.3$ and 0.4. The sign of peaks in the XMCD spectra represents the direction of local magnetic moments. In the XMCD spectra shown in Fig. 2(a), the positive peak and the negative peak were observed at 934 eV and 955 eV, respectively. On the other hand, they are reversed in Fig. 2(b), meaning the reversal of the magnetic moment of Cu atoms. Both the minimum magnetization and the reversal of the magnetic moment appear when the MC occurs. On the basis of these results, we conclude that there is an MC composition at RT in $Mn_{4-x}Cu_xN$ films between $x = 0.3$ and 0.4.

[Acknowledgment] The XAS and XMCD measurements were performed with the approval of the Photon Factory Program Advisory Committee (Proposal No. 2022G036).

[Reference]

[1] T. Komori *et al.*, J. Appl. Phys. **127**, 043903 (2020).
[2] H. Mitarai *et al.*, Phys. Rev. Mater. **4**, 094401 (2020).
[3] S. Ghosh *et al.*, Nano Lett. **21**, 2580 (2021).
[4] R. Zhang *et al*., Acta Mater. **234**, 118021 (2022).

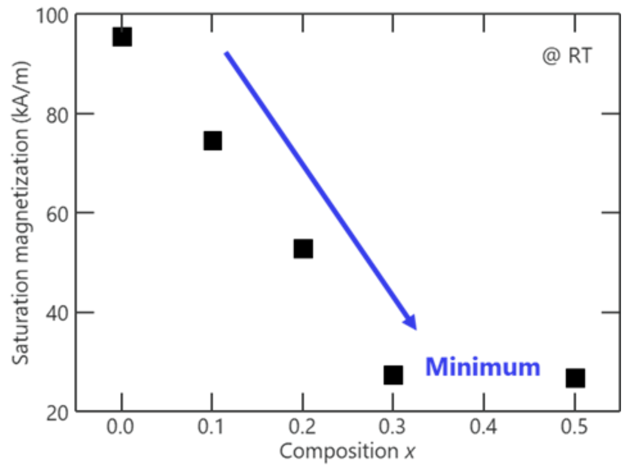

Fig. 1. Composition dependence of saturation magnetization.

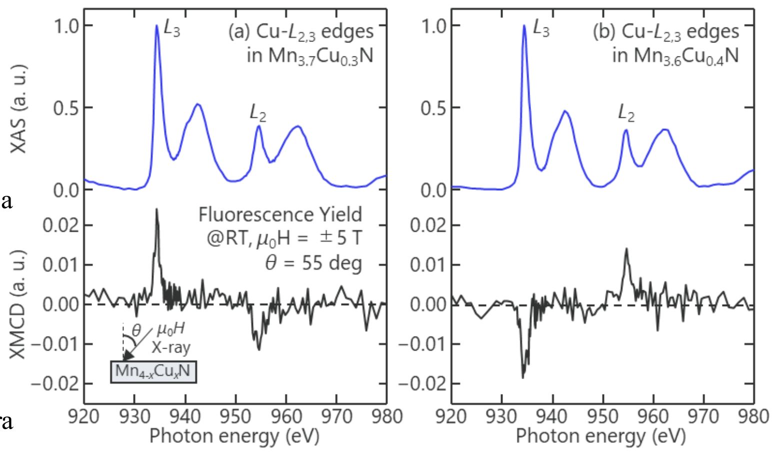

Fig. 2. XAS and XMCD spectra in (a) $Mn_{3.7}Cu_{0.3}N$ and (b) $Mn_{3.6}Cu_{0.4}N$ films at Cu-$L_{2,3}$ edges (XAS are standardized.)

PLD 法による(100)MgO 上の磁性 GdN 薄膜の結晶方位制御

Crystal orientation control of ferromagnetic GdN thin film on (100) MgO by PLD

[1]NTT 物性研、[2]東北大学、[3]広島大学 ○田中 祐輔[1]、Yoshiharu Krockenberger[1]、国橋 要司[1]、新田 淳作[1,2]、後藤 秀樹[1,3]、眞田 治樹[1]

[1]NTT-BRL , [2]Tohoku Univ., [3]Hiroshima Univ. ○Yusuke Tanaka[1], Yoshiharu Krockenberger[1], Yoji Kunihashi[1], Junsaku Nitta[1,2], Hideki Gotoh[1,3] and Haruki Sanada[1]

E-mail: yusukedy.tanaka@ ntt.com

GdN has attracted much attention as a ferromagnetic insulator whose Curie temperature (T_C ~ 70 K) is highest among rare earth nitrides [1]. Furthermore, it is predicted that GdN, grown in the (100) direction, becomes a Chern insulator [2]. Although there are several reports on the growth of (111) GdN [3], few on (001) film. Here, we investigated crystal growth of GdN thin film by pulsed laser deposition and found that the orientation of GdN thin films can be controlled via a TiN buffer layer. We used a sintered target of GdN powder and grew GdN on (001) MgO substrates in a nitrogen atmosphere. All GdN films were covered with a 50-100 nm TiN capping layer to avoid deliquescence (Fig. 1). When we grew it directly on (001) MgO substrates at 900 °C, (111) GdN films were obtained as indicated by the X-ray diffraction spectrum in Fig. 2. Measurement of *M*-*T* curve for the (111) GdN / (001) MgO films with applying magnetic field perpendicular to the growth direction showed the Curie temperature of the (111) GdN was T_C~70 K. When we inserted TiN buffer layer between GdN and MgO, (001) GdN films were obtained (red curve in Fig. 2). We also confirmed the high quality of TiN buffer layer with Laue fringes in the X-ray diffraction spectra is important to obtain (001) GdN films with uniformly oriented crystal. Our results indicate that this technique is useful for the synthesis of (001) GdN films with high crystal quality, which is necessary for the realization of the Chern insulators. This work was partly supported by JSPS KAKENHI Grant Number JP23H01792.

[1] D. Massarotti *et al.*, Nat. Commun. **6**, 7376 (2015).
[2] Z. Li *et al.*, Phys. Rev. B **92**, 201303(R) (2015).
[3] H. Yoshitomi *et al.*, Phys. Rev B **83**, 155202 (2011).

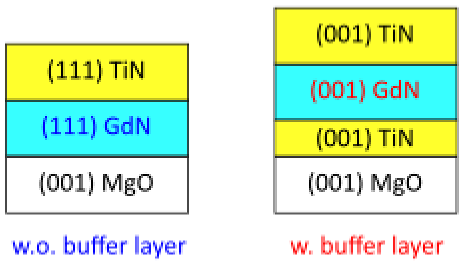

Fig. 1 Schematic view of synthesized device structure.

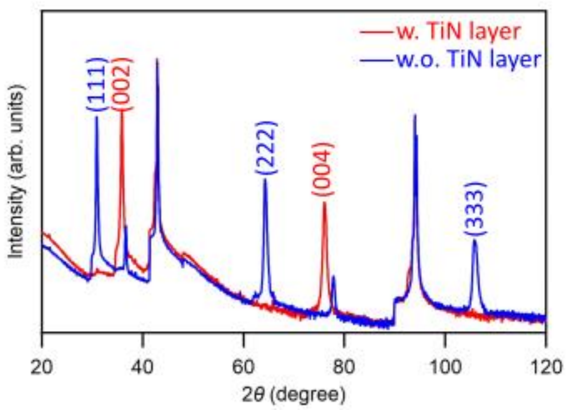

Fig. 2 θ-2θ scan of GdN thin film on (100) MgO substrate with/without TiN buffer layer.